REPORT DOCUMENTATION PAGE

Form Approved
OMB No. 0704-0188

1. REPORT DATE *(DD-MM-YYYY)*	2. REPORT TYPE	3. DATES COVERED *(From - To)*
30-09-2011	Performance/Technical Report (Final)	Jan. 2010 - Sept. 2011

4. TITLE AND SUBTITLE
Robust High Data Rate MIMO Underwater Acoustic Communications

5a. CONTRACT NUMBER

5b. GRANT NUMBER
N00014-10-1-0054

5c. PROGRAM ELEMENT NUMBER

6. AUTHOR(S)
Jian Li

5d. PROJECT NUMBER

5e. TASK NUMBER

5f. WORK UNIT NUMBER

7. PERFORMING ORGANIZATION NAME(S) AND ADDRESS(ES)
University of Florida
Office of Engineering Research
343 Weil Hall, P.O.Box 116550
Gainesville, FL 32611

8. PERFORMING ORGANIZATION REPORT NUMBER

9. SPONSORING/MONITORING AGENCY NAME(S) AND ADDRESS(ES)
Office of Naval Research
875 North Randolph Street
Arlington, VA 22203-1995

10. SPONSOR/MONITOR'S ACRONYM(S)
ONR

11. SPONSORING/MONITORING AGENCY REPORT NUMBER

12. DISTRIBUTION AVAILABILITY STATEMENT
Approved for Public Release; Distribution is Unlimited.

13. SUPPLEMENTARY NOTES

14. ABSTRACT
Our research focuses on mobile multi-input multi-output communications over sparse acoustic channels subject to both inter-symbol interference and Doppler scaling effects. Temporal resampling is implemented to effectively convert the Doppler scaling effects to Doppler frequency shifts. We evaluate two practical channel models and compare the performance of the corresponding channel estimation algorithms, namely, the generalization of the sparse learning via iterative minimization (GoSLIM) algorithm and its variation, GoSLIM-V. For symbol detection, we consider the Turbo equalization schemes implemented by the linear minimum mean-squared error based soft-input soft-output equalizer and its low complexity approximation, respectively. The latter provides only slightly degraded detection performance at a significantly lower computational complexity compared to the former.The effectiveness of the considered approaches is verified using the WHOI09, ACOMM10, and MACE10 experimental results.

15. SUBJECT TERMS
Mobile underwater acoustic communications, multi-input multi-output, Doppler effects, inter-symbol interference, temporal resampling, generalization of the sparse learning via iteratvie minimication, Turbo equalization

16. SECURITY CLASSIFICATION OF:			17. LIMITATION OF ABSTRACT	18. NUMBER OF PAGES	19a. NAME OF RESPONSIBLE PERSON
a. REPORT	b. ABSTRACT	c. THIS PAGE			Jian Li
U	U	U	UU	24	19b. TELEPONE NUMBER *(Include area code)* (352) 392-2642

Robust High Data Rate MIMO Underwater Acoustic Communications

Jian Li
P.O. Box 116130, Dept. of ECE, Univ. of Florida, Gainesville, FL 32611
phone: (352) 392-2642 fax: (352) 392-0044 email: li@dsp.ufl.edu

Award Number: N00014-10-1-0054
http://www.sal.ufl.edu

LONG-TERM GOALS

Achieving reliable communications with high data rates over underwater acoustic communication (UAC) channels has long been recognized as a challenging problem owing to the scarce bandwidth available and the time-varying channels with large delay spread. Fortunately, the underwater environment with multipath scattering makes it possible for multi-input multi-output (MIMO) spatial multiplexing schemes to achieve high data rate UAC. The major challenges of the high data rate MIMO UAC scheme include time-varying channels, long delay spreads, mutual interferences among the data streams transmitted by the different transducers, and Doppler scaling effects due to relative movement between transmitter and receiver platforms. These challenges require short and effective training sequences, reliable temporal resampling schemes, efficient channel estimation and tracking algorithms, and innovative equalization and decoding strategies. Our long-term goals are to efficiently and effectively tackle these challenges.

OBJECTIVES

The objectives of our proposed research are: 1) to synthesize effective and efficient training sequences with cyclic prefixes for the accurate estimation and prediction of UAC channels, 2) to develop a temporal resampling scheme that can sufficiently compensate for the Doppler scaling effects, 3) to devise robust and computationally efficient sparse channel estimation and tracking algorithms that can be used to provide statistical properties of the estimated UAC channels, 4) to design efficient detection scheme that can effectively perform interference cancellation in a MIMO system, and to provide channel updating, equalization, and decoding schemes with good initial conditions to allow improved turbo processing, and 5) to continue the ongoing in-water experimentation and algorithm evaluation activities by continuing our collaborations with the Woods Hole Oceanographic Institution (WHOI) and others.

APPROACH

Training sequence design: We have recently introduced a new cyclic algorithm (called CAN = CA-New) for the local minimization of the integrated sidelobe level (ISL) metric for efficient aperiodic sequence designs. CAN is based on fast Fourier transform (FFT) operations and can be used virtually for any practically relevant values of the sequence length, which can be up to a million or even larger. We have also extended CAN to generate perfect periodic sequences, which are the so-called constant

amplitude zero auto-correlation (CAZAC) sequences. This CAZAC sequence design problem goes back to Norbert Wiener or even Gauss! The mathematicians have shown that for some sequence lengths, there are an infinite number of perfect periodic sequences. We have solved a long-standing perfect periodic sequence design problem – finding such sequences (including long sequences) efficiently and effectively. We solved it via exploiting FFTs.

The extended CAN algorithm is referred to as periodic CAN (PeCAN). Unlike most existing sequence construction methods which are algebraic and deterministic in nature, we start the iteration of PeCAN from random phase initializations and then proceed to cyclically minimize the desired metric. In this way, through different random phase initializations, we can find as many different waveforms as we may ever want! The so-generated sequences are difficult to guess by the foe and hence are especially useful as training sequences or as spreading sequences for covert UAC applications. We will use PeCAN sequences for more in-water experimentations to demonstrate their effectiveness.

Temporal Resampling: In mobile MIMO UAC, the presence of Doppler effects, owing to the relative motions between the transmitter and receiver platforms, induces temporal scaling (stretching or compression) to the transmitted signals. The Doppler scaling effects can be sufficiently compensated for by converting the original acoustic channel subject to both inter-symbol interference (ISI) and Doppler scaling effects to an ISI channel via resampling the received measurements. Although the Doppler scaling effects can be largely mitigated after such a temporal resampling process, the residual Doppler still causes frequency shift on the received measurements, which requires the employment of channel estimation algorithm that can accurately estimate the resulting frequency modulated acoustic channel.

Channel Estimation: Through simultaneous transmissions using multiple transmitters, MIMO systems offer enhanced reliability and/or increased data rates compared to their single-input counterparts. However, in MIMO systems, the multiple transmissions lead to mutual interferences at the receiver. To successfully recover the transmitted data sequences, accurate channel estimation techniques play crucial roles. We focus on MIMO UAC over sparse acoustic channels suffering from ISI and frequency modulations. We first present an extension of our recently introduced SLIM algorithm, which stands for Sparse Learning via Iterative Minimization, to estimate the sparse and frequency modulated acoustic channels. The extended algorithm is referred to as generalization of SLIM (GoSLIM). GoSLIM assumes that at each receiver, the channel taps for all the transmitters experience the same Doppler frequency, but different receivers experience different Doppler shifts. We further simplify this channel model by assuming that the channel taps for all the transmitter and receiver pairs experience the same Doppler frequency. Accordingly, a variation of GoSLIM, referred to as GoSLIM-V (V stands for variation), is presented. We show that compared to GoSLIM, GoSLIM-V not only reduces the overall complexity involved in the channel estimation stage, but also slightly improves the detection performance. This comparison between GoSLIM and GoSLIM-V suggests that proper channel modeling is critical for effective and efficient mobile MIMO UAC.

Receiver Design: The channel-induced phase shift should be first compensated for using the Doppler frequency estimate. Such phase compensation task, along with the aforementioned temporal resampling process, effectively converts an acoustic channel subject to both ISI and Doppler scaling effects to an ISI channel, which allows for the employment of various equalization techniques that can effectively combat ISI. We use a linear minimum mean-squared error (LMMSE) based filter for symbol detection. In a MIMO setup, on top of ISI, multiple simultaneously transmitted signals act as interferences to one another. Therefore, interference cancellation scheme also plays a critical role in

the overall detection performance. A hard decision based interference cancellation scheme, including vertical BLAST (V-BLAST) and RELAX-BLAST, subtracts the hard decisions of detected signals out from the received measurements to aid the detection of the remaining signals. By combining V-BLAST with the cyclic principle of the RELAX algorithm, RELAX-BLAST provides superior detection performance over V-BLAST at the cost of slightly increased complexities.

The detection performance can be further enhanced by employing a soft interference cancellation scheme, including Turbo equalization. For a receiver employing Turbo equalization, both the equalizer and decoder involved are configured as soft-input soft-output. The detection performance improves as the soft information cycles between the equalizer and decoder. The main drawback of the Turbo equalization scheme is the increased computational complexity compared to its hard decision based counterparts. To address this problem, we consider a low complexity approximation of soft-input soft-output equalizer, which enjoys a computational complexity comparable to RELAX-BLAST and provides only slightly degraded detection performance compared to a directly implemented equalizer.

WORK COMPLETED

The received measurements should be first temporally resampled to mitigate the Doppler scaling effects. We take advantage of the preamble and the postamble of a data packet to estimate the Doppler scaling factor via channel estimation. Specifically, by using a channel estimation algorithm for acoustic channels suffering from Doppler scaling effects, we can obtain the channel impulse responses (CIRs) from the two measurement segments in response to the preamble and postamble. The time duration change $\hat{T}_d$ imposed on the packet can be inferred from the tap shift of the principal arrivals of these two CIRs. Then the Doppler scaling factor estimate is computed as $\hat{\beta} = \frac{T_{tx} + \hat{T}_d}{T_{tx}}$, where T_{tx} represents the duration of the same packet at the transmitter side. Since $\hat{\beta}$ can never be perfectly accurate, after temporal resampling, Doppler frequency shifts still exist. Accordingly, the resulting acoustic channels can be reasonably modeled as frequency modulated channels.

By extending the SLIM algorithm to deal with Doppler frequency modulation, we have devised the GoSLIM algorithm to estimate the underlying CIRs and Doppler frequency in a joint manner. Before proceeding to discuss GoSLIM, it is instructive to review a simpler case, i.e., the channel estimation problem in stationary channels using the SLIM algorithm. We consider a MIMO UAC system equipped with N transmitters and M receivers. For stationary frequency-selective channels, the channel estimation problem at the m^{th} receiver is given by $\mathbf{y}_m = \sum_{n=1}^{N} \mathbf{X}_n \mathbf{h}_{n,m} + \mathbf{e}_m$, where $\mathbf{y}_m$ is the received measurement vector, $\mathbf{X}_n$ is constructed using the training sequences in the training-directed mode or the previously detected symbols in the decision-directed mode, $\mathbf{h}_{n,m} = [h_{n,m,1}, ..., h_{n,m,R}]^T$ characterizes the CIR of length of R between the n^{th} transmitter and the m^{th} receiver, and $\mathbf{e}_m$ is the additive noise. The channel estimation problem can be expressed more compactly as $\mathbf{y}_m = \bar{\mathbf{X}} \mathbf{h}_m + \mathbf{e}_m$, where $\bar{\mathbf{X}} = [\mathbf{X}_1, ..., \mathbf{X}_N]$ and $\mathbf{h}_m = [\mathbf{h}_{1,m}^T, ..., \mathbf{h}_{N,m}^T]^T$. We consider SLIM for estimating $\mathbf{h}_m$ given $\mathbf{y}_m$ and $\bar{\mathbf{X}}$ and assume that the noise vector $\mathbf{e}_m$ contains a circularly symmetric independent and identically

distributed (i.i.d.) complex-valued Gaussian random variables with zero-mean and variance η_m. Let $p_{n,m,r}$ be the variance of $h_{n,m,r}$, and define $\mathbf{p}_{n,m} = [p_{n,m,1}, ..., p_{n,m,R}]^T$ and $\mathbf{p}_m = [\mathbf{p}_{1,m}^T, ..., \mathbf{p}_{N,m}^T]^T$. Define $\mathbf{P}_m = \text{diag}(\mathbf{p}_m)$ as the covariance matrix of the channel taps seen by the m^{th} receiver and $\mathbf{x}_{n,m,r}$ as the column of $\bar{\mathbf{X}}$ that corresponds to $h_{n,m,r}$. SLIM is user parameter free, making it easy to use in practice. The SLIM algorithm can be implemented as:

- Step 0: Initialize $h_{n,m,r} = \dfrac{\mathbf{x}_{n,m,r}^H \mathbf{y}}{\mathbf{x}_{n,m,r}^H \mathbf{x}_{n,m,r}}$.
- Step 1: With the most recent $\mathbf{h}_m$, calculate $p_{n,m,r} = \left|h_{n,m,r}\right|^2$.
- Step 2: With the most recent $\mathbf{P}_m$ and η_m, calculate $\mathbf{h}_m = \left(\bar{\mathbf{X}}^{\mathrm{H}} \bar{\mathbf{X}} + \eta_m \mathbf{P}_m^{-1}\right)^{-1} \bar{\mathbf{X}}^{\mathrm{H}} \mathbf{y}_m$.
- Step 3: With the most recent $\mathbf{h}_m$, update, $\eta_m = \dfrac{\left\|\mathbf{y}_m - \bar{\mathbf{X}}\mathbf{h}_m\right\|^2}{d_y}$, where d_y denotes the length of $\mathbf{y}_m$.
- Iterate Steps 1-3 until convergence.

For frequency-selective channels further modulated by a Doppler frequency f_m at the m^{th} receiver, the channel estimation problem becomes $\mathbf{y}_m = \mathbf{\Lambda}_m \bar{\mathbf{X}} \mathbf{h}_m + \mathbf{e}_m$. The vectors $\mathbf{y}_m$, $\mathbf{h}_m$, and $\mathbf{e}_m$ have already been defined previously and $\mathbf{\Lambda}_m = \text{diag}\left(1, e^{-2j\pi f_m T_s}, \cdots, e^{-2j\pi f_m T_s (d_y - 1)}\right)$ represents the Doppler shift matrix. In $\mathbf{\Lambda}_m$, f_m is the Doppler frequency to be estimated and T_s represents the symbol period. Given $\mathbf{y}_m$ and $\bar{\mathbf{X}}$, we consider the extension of the SLIM algorithm, referred to as generalization of SLIM (GoSLIM) to estimate the CIR $\mathbf{h}_m$ and the underlying Doppler frequency f_m jointly. The GoSLIM algorithm can be implemented as:

- Step 0: Initialize $h_{n,m,r} = \dfrac{\mathbf{x}_{n,m,r}^H \mathbf{y}}{\mathbf{x}_{n,m,r}^H \mathbf{x}_{n,m,r}}$ and $f_m = 0$.
- Step 1: With the most recent $\mathbf{h}_m$, calculate $p_{n,m,r} = \left|h_{n,m,r}\right|^2$.
- Step 2: With the most recent $\mathbf{\Lambda}_m$, $\mathbf{P}_m$, and η_m, calculate $\mathbf{h}_m = \left(\bar{\mathbf{X}}^{\mathrm{H}} \bar{\mathbf{X}} + \eta_m \mathbf{P}_m^{-1}\right)^{-1} \left(\mathbf{\Lambda}_m \bar{\mathbf{X}}\right)^{\mathrm{H}} \mathbf{y}_m$.
- Step 3: With the most recent $\mathbf{h}_m$, we calculate $\tilde{\mathbf{x}}_m = \bar{\mathbf{X}}\mathbf{h}_m$. Denote $\tilde{x}_m(i)$ and $y_m(i)$ as the i^{th} element of $\tilde{\mathbf{x}}_m$ and $\mathbf{y}_m$, respectively. Then, the Doppler frequency can be calculated as $f_m = \arg\max_{f_m} \text{Re}\left(\sum_{i=1}^{d_y} z_m(i) e^{-2j\pi f_m T_s (i-1)}\right)$, where $z_m(i) = y_m^*(i)\tilde{x}_m(i)$.
- Step 4: With the most recent $\mathbf{\Lambda}_m$ and $\mathbf{h}_m$, calculate $\eta_m = \dfrac{\left\|\mathbf{y}_m - \mathbf{\Lambda}_m \bar{\mathbf{X}} \mathbf{h}_m\right\|^2}{d_y}$.
- Iterate Steps 1-4 until convergence.

The channel estimation problem $\mathbf{y}_m = \mathbf{\Lambda}_m \bar{\mathbf{X}} \mathbf{h}_m + \mathbf{e}_m$ corresponds to an assumption that the NR channel taps seen by the m^{th} receiver experience the same Doppler frequency f_m, but the frequency value could vary at different receive hydrophones. We consider a further simplified assumption that the

Doppler frequency is the same across M receivers, i.e., $f = f_1 = \cdots = f_M$. Accordingly, replacing f_m in the Doppler shift matrix $\mathbf{\Lambda}_m$ by f yields a matrix $\bar{\mathbf{\Lambda}} = \mathrm{diag}\left(1, e^{-2j\pi f T_s}, \cdots, e^{-2j\pi f T_s (d_y - 1)}\right)$ that is independent of the receiver index m. Accordingly, the measurements at the m^{th} receiver can be expressed as $\mathbf{y}_m = \bar{\mathbf{\Lambda}}\bar{\mathbf{X}}\mathbf{h}_m + \mathbf{e}_m$. Stacking the measurements from all the receivers follows $\mathbf{y} = \mathbf{\Lambda}\mathbf{X}\mathbf{h} + \mathbf{e}$, where $\mathbf{y} = [\mathbf{y}_1^T, ..., \mathbf{y}_M^T]^T$, $\mathbf{h} = [\mathbf{h}_1^T, ..., \mathbf{h}_M^T]^T$, $\mathbf{e} = [\mathbf{e}_1^T, ..., \mathbf{e}_M^T]^T$, $\mathbf{\Lambda} = \mathbf{I}_{M \times M} \otimes \bar{\mathbf{\Lambda}}$, and $\mathbf{X} = \mathbf{I}_{M \times M} \otimes \bar{\mathbf{X}}$ ($\mathbf{I}$ denotes an identiy matrix and $\otimes$ denotes the Kronecker product). Again, we assume that $\mathbf{e}$ contains circularly symmetric i.i.d. complex-valued Gaussian random variables with zero-mean and variance η. Then, the variation of GoSLIM, referred to as GoSLIM-V, aims to estimate f and $\mathbf{h}$ given $\mathbf{y}$ and $\mathbf{X}$. Note that unlike GoSLIM, which can be employed at each receiver to estimate the channel in parallel, GoSLIM-V implicitly suggests that the measurements acquired at different receivers should be assembled in a central processor before performing channel estimation. Moreover, GoSLM-V simultaneously estimates the CIRs among all of the MN transmitter and receiver pairs. The GoSLIM-V algorithm can be implemented as:

- Step 0: Initialize $h_{n,m,r} = \dfrac{\mathbf{x}_{n,m,r}^H \mathbf{y}}{\mathbf{x}_{n,m,r}^H \mathbf{x}_{n,m,r}}$ and $f = 0$.
- Step 1: With the most recent $\mathbf{h}$, calculate $p_{n,m,r} = \left|h_{n,m,r}\right|^2$.
- Step 2: With the most recent $\mathbf{\Lambda}$, $\mathbf{P}$ and η, calculate $\mathbf{h} = \left(\mathbf{X}^{\mathrm{H}}\mathbf{X} + \eta\mathbf{P}^{-1}\right)^{-1}(\mathbf{\Lambda}\mathbf{X})^{\mathrm{H}}\mathbf{y}$.
- Step 3: With the most recent $\{\mathbf{h}_m\}_{m=1}^M$, we calculate $\tilde{\mathbf{x}}_m = \bar{\mathbf{X}}\mathbf{h}_m$. Denote $\tilde{x}_m(i)$ and $y_m(i)$ as the i^{th} element of $\tilde{\mathbf{x}}_m$ and $\mathbf{y}_m$, respectively. Then, the Doppler frequency can be calculated as $f = \arg\max_f \mathrm{Re}\left(\sum_{i=1}^{d_y}\left(\sum_{m=1}^{M} z_m(i)\right)e^{-2j\pi f T_s (i-1)}\right)$, where $z_m(i) = y_m^*(i)\tilde{x}_m(i)$.
- Step 4: With the most recent $\mathbf{\Lambda}$ and $\mathbf{h}$, calculate $\eta = \dfrac{\left\|\mathbf{y} - \mathbf{\Lambda}\mathbf{X}\mathbf{h}\right\|^2}{Md_y}$.
- Iterate Steps 1-4 until convergence.

Empirical experience indicates that the computational bottleneck of both GoSLIM and GoSLIM-V is in the update of the Doppler frequency. Since GoSLIM is employed at each receiver to conduct Doppler frequency estimation in parallel while GoSLIM-V estimates the common Doppler frequency across M receivers, M times complexity reduction is achieved by employing GoSLIM-V when updating the Doppler frequency estimation. As a consequence, GoSLIM-V is computationally much more efficient than GoSLIM in a MIMO configuration, especially with a large number of receive elements. Due to the reduced number of unknowns, the GoSLIM-V data model is more parsimonious than that of GoSLIM, which could enhance the symbol detection performance if the model is reasonably accurate.

For Doppler modulated frequency-selective channels, once the estimate of the Doppler frequencies $\{f_m\}_{m=1}^M$ (or Doppler frequency f) is available, the receiver can compensate out the adverse effects induced by the Doppler shift and effectively convert the original frequency-modulated channels to stationary frequency-selective channels. This way, various reception schemes that are effective for stationary frequency-selective channels can be applied. In particular, we consider both spatial

multiplexing schemes including RELAX-BLAST and Turbo equalization, and space-time coding schemes including Alamouti diversity techniques.

Although Turbo equalization significantly improves the detection performance compared to its RELAX-BLAST counterpart, its computational complexity is much more expensive than RELAX-BLAST mainly because to calculate the LMMSE filter coefficients, we need to perform matrix inversion at each time index. To address this problem, we consider a low complexity approximation of the exact LMMSE based Turbo equalizer, where the approximate LMMSE filters have constant coefficients over one symbol block. We shown that Turbo equalization employing such low complexity equalizer yields slightly degraded detection performance compared to that adapting a directly implemented equalizer, and this is achieved at a computational complexity comparable to RELAX-BLAST. We hereafter refer to the Turbo equalization scheme that employs a directly implemented equalizer as "Exact-LMMSE-Turbo" and its low complexity approximation as "Approximate-LMMSE-Turbo".

RESULTS

1. WHOI09 Experimental Results

The WHOI09 in-water experiment was conducted in December 2009. The 4 transmit transducers with source spacing up to 1 m were suspended from a vessel heaving in a 14 m mid-depth water column. Two separate 4-hydrophone arrays were deployed approximately 1 km and 2 km away from the source array and they will be referred to, respectively, as RB1 and RB2 receiving arrays. Both RB1 and RB2 receiving arrays had 0.21 m spacing between adjacent hydrophones, and they were mounted on an anchored buoy in a mid-water column during the course of data collection. The Doppler shift was mainly caused by the relative motion between the transmitters and receivers. The carrier frequency, the sampling frequency, and the symbol rate employed in WHOI09 experiment were 30 KHz, 200 KHz, and 8 KHz, respectively.

GoSLIM is employed to estimate the underlying CIRs and Doppler frequencies by making use of the shifted PeCAN training sequences periodically allocated in the transmitted sequence. Figure 1 shows the CIR evolution between the active transmitter and the 2nd hydrophone for all the 6 epochs (the reason why we consider the 2nd hydrophone will be explained shortly). One observes that the position of the principal arrival shown in Figure 1 slowly shifts with time due to the fact that the transmitter array was suspended from a vessel heaving in a water column and the receiving hydrophone arrays were mounted on anchored buoys during the course of data collection. Figure 2, on the other hand, plots the evolution of the Doppler frequency for each hydrophone. The reverberating Doppler frequency estimates obtained from the GoSLIM algorithm shows the presence of Doppler shifts.

Space-time coding schemes: Alamouti coding

To investigate the performance of 2Tx-1Rx Alamouti code, the structure of the transmitted sequences is shown in Figure 3. Two synchronized transmitters were used. Each transmitter sent 4 data packets and each data packet was divided into 16 blocks followed by a gap to ensure the absence of inter-packet interferences. In our design, each payload segment, (e.g., **a** or **b** in Figure 3), contains 250 coded QPSK symbols. Taking the segment **a** for example, it is generated, as shown in Figure 3, by feeding 250 source bits into a 1/2 rate convolutional encoder followed by a random interleaver and

QPSK modulation. Segment **b**, as well as the segments in other blocks, is similarly generated but with different realizations of the source bits and random interleaver. The resulting uncoded and coded data rates are 7 kbps and 3.5 kbps, respectively.

Since each payload block contains a training sequence as shown in Figure 3, the reception scheme for each block is performed as follows: the receiver first conducts training-directed channel estimation (note that the GoSLIM and GoSLIM-V algorithms are identical in this case since only one receiver is involved) by making use of the training sequence, and then detects the payload symbols contained in the two payload segments before and after the training sequence. As a consequence, decision-directed estimation is not needed. For the sequence in Figure 3, each block carries 500 QPSK payload symbols. Therefore each epoch carries 32 k symbols (or equivalently, 64 k uncoded bits or 32 k coded bits) and we have 3 epochs for each receiving array. The channel tap number is fixed at 30 for all epochs. The BER results at different receive hydrophones, by averaging over 192 k uncoded bits and 96 k coded bits, are summarized in Table I for each receiving array. One observes from Table I that the 2nd hydrophone of RB1 array yields remarkably high BERs. This can be explained by the fact that the power of the channel estimate at this hydrophone is persistently lower than that at other hydrophones by almost an order of magnitude, which is evidenced in Figure 1.

Spatial multiplexing schemes: BLAST data

We also designed 4-input BLAST data packet, which attained a coded data rate of 30 kbps by leveraging the MIMO scheme. The payload sequence was divided into blocks, each of length 250, and each block was encoded using a ½ convolutional encoder with constraint length 5. The source information is a grayscale Gator mascot shown in Figure 4(a). We made full use of the available resources by transmitting 4 sequences simultaneously and incorporating the measurements acquired from all the 4 hydrophones, establishing a 4×4 MIMO system. With the RELAX-BLAST scheme employed in the symbol detection stage, we first compare the resulting BER performance of the GoSLIM and GoSLIM-V algorithms in the channel estimation stage. When GoSLIM is employed, Figures 4(b), 4(c), and 4(d) show the recovered grayscale mascots for epochs "195600", "195730", and "195860", respectively. The corresponding coded BERs and the computational time consumed at the channel estimation stage on an ordinary workstation (Intel Xeon E5506 processor 2.13G Hz, 12GB RAM, Windows 7 64-bit, and MATLAB R2010b) are listed in the first row of Tables 2 and 3, respectively. In comparison, when GoSLIM-V is employed, the recovered grayscale mascots are shown in Figures 4(e), 4(f), and 4(g), with the corresponding BERs and computational complexities listed in the second row of Tables 2 and 3, respectively. One observes from Table 2 that GoSLIM-V yields slightly better BER results than its GoSLIM counterpart. Moreover, Table 3 demonstrates that GoSLIM-V is about 4 times faster than GoSLIM. Due to the advantage of GoSLIM-V over the original GoSLIM algorithm, we hereafter employ GoSLIM-V in the channel estimation stage and compare the RELAX-BLAST scheme with the Turbo equalization counterpart in the symbol detection stage.

We remark that the three grayscale mascots carried by epochs "195600", "195730", and "195860", respectively, can be perfectly recovered by employing either type of the Turbo equalization scheme. Moreover, Table 4 lists the ratio of the time consumed to process a packet to the duration of the same packet during transmission, obtained using Exact-LMMSE-Turbo, Approximate-LMMSE-Turbo, and the RELAX-BLAST scheme, respectively. The results are obtained by applying 3 iterations for all of the three types of detection schemes considered.

2. ACOMM10 Experimental Results

The ACOMM10 experiment took place in July 2010 in the Mid-Atlantic Bight on the continental shelf off the coast of New Jersey in an area with water depth of 78 m. The transmitter array consisted of 12 transducers with 0.8 m spacing between adjacent elements. In our design, only 4 transducers were activated. The receiving array was composed of 8 hydrophones. The spacing between the adjacent hydrophones was 2.06 m except the first element, which was spaced 4 m above the second element. Both the transmit array and the receiving array were mounted on anchored buoys and were deployed approximately 3 km away from each other. The Doppler shift was mainly caused by the relative motion between the transmitters and receivers. The carrier frequency, the sampling frequency, and the symbol rate employed in the ACOMM10 experiment were 20 kHz, 80 kHz, and 4 kHz, respectively.

The BLAST data package of 20 s in duration was transmitted multiple times in the ACOMM10 experiment and was recorded by the receiving array. A total of 89 epochs were available and they are referred to as "MIMO01"--"MIMO89", respectively. Figures 5 and 6 show, respectively, the evolutions of CIR and Doppler frequencies estimated by GoSLIM. The position shift of the principal arrival with respect to time shown in Figure 5 and the reverberating Doppler frequency estimates shown in Figure 6 suggest the presence of the Doppler shifts.

Spatial multiplexing schemes: BLAST data

Figure 7 shows the source information contained in the transmitted package. Each package consists of 7 packets. The first 4 packets convey 4 grayscale Gator mascots and the last 3 packets combined form a colored mascot. The RGB components of the colored image are transmitted in the 5^{th}, 6^{th}, and 7^{th} packets, respectively. Guard intervals between adjacent packets are used to prevent inter-packet interference. Each pixel of the grayscale image is represented by 5 bits, corresponding to 32 different intensities (e.g., pure white and pure dark pixels are represented by 11111 and 00000, respectively). The 64-pixel by 100-pixel grayscale mascot image, as a consequence, is represented by a total of 32 k source bits. (Accordingly, a colored mascot image is represented by 96 k bits.) The contrast of the grayscale image, as well as the hue of the colored image, has been carefully adjusted so that the image carries approximately equal numbers of 1's and 0's. The source information obtained from the Gator mascots was divided into blocks, each of length 250, and each block was encode using a ½ convolutional encoder with constraint length 5. By transmitting $N = 4$ sequences simultaneously and incorporating the measurements acquired from all of the $M = 8$ receiver elements for analysis, we established a 4×8 MIMO UAC system, which leads to a net coded data rate of 15 kbps.

We first assess the impact of the channel estimation algorithm (GoSLIM or GoSLIM-V) on the resulting detection performance. With the estimated CIRs and Doppler frequency (frequencies), after phase compensation, the payload symbols are detected using the RELAX-BLAST scheme. There is a total of 623 packets (recall that we have 89 epochs and each consists of 7 packets) available and we deem a packet to be successfully detected if its coded BER is less than 0.1. When GoSLIM is employed as the channel estimation algorithm, we have succeeded in tracking the entire 32 payload blocks for 594 packets. A coded BER of 5.1×10^{-3} is achieved after averaging over the 594 successful packets. In comparison, when GoSLIM-V is used, 599 packets are successfully retrieved with an average coded BER of 4.9×10^{-3}. We use the 1^{st} packet (i.e., the one conveys a grayscale gator mascot; see Figure 7) of three epochs, namely "MIMO02", "MIMO06", and "MIMO18", to compare the impact of the two channel estimation algorithms on the resulting BER performance and computation complexity. When GoSLIM is employed, Figures 8(a), 8(b), and 8(c) show the recovered grayscale

mascots for "MIMO02", "MIMO06", and "MIMO18", respectively. The corresponding coded BERs and the computational time consumed at the channel estimation stage on an ordinary workstation (Intel Xeon E5506 processor 2.13G Hz, 12GB RAM, Windows 7 64-bit, and MATLAB R2010b) are listed in the first row of Tables 5 and 6, respectively. In comparison, when GoSLIM-V is employed, the recovered grayscale mascots are shown in Figures 8(d), 8(e), and 8(f), with the corresponding BERs and computational complexities listed in the second row of Tables 5 and 6, respectively. One observes from Table 5 that GoSLIM-V yields slightly better BER results than its GoSLIM counterpart. Moreover, Table 6 demonstrates that GoSLIM-V is about 4 times faster than GoSLIM. Due to the advantage of GoSLIM-V over the original GoSLIM algorithm, we hereafter employ GoSLIM-V in the channel estimation stage and compare the RELAX-BLAST scheme with the Turbo equalization counterpart in the symbol detection stage.

Table 7 lists the successfully detected packet percentage, the error-free packet percentage, the coded BER averaged over the successful packets, and the time ratio of the time consumed to process a packet to the duration of the same packet during transmission, obtained using Exact-LMMSE-Turbo, Approximate-LMMSE-Turbo, and the RELAX-BLAST scheme, respectively. The results are obtained by applying 3 iterations for all of the three types of detection schemes considered. One observes from Table 7 that 1) BER-wise, both Exact-LMMSE-Turbo and Approximate-LMMSE-Turbo outperform RELAX-BLAST significantly, 2) Approximate-LMMSE-Turbo greatly reduces the complexity at the cost of slight BER performance degradation compared to Exact-LMMSE-Turbo, and 3) compared to RELAX-BLAST, Approximate-LMMSE-Turbo improves the BER performance by two orders of magnitude without significantly increasing the computational complexities.

3. MACE10 Experimental Results

The MACE10 in-water experiment was conducted off the coast of Martha's Vineyard, MA in June 2010. A source array consisting of 4 transducers was vertically deployed at a depth of 80 m, and towed by a vessel. At the receiver side, a 12-element hydrophone array was mounted on a buoy. The vessel moved from the minimum range of 500 m away from the receiving array outbound to the maximum range of 4000 m and then inbound back to the minimum range. The carrier frequency, the sampling frequency, and the symbol rate employed in the MACE10 experiment were 13 kHz, 39.0625 kHz, and 3.90625 kHz, respectively. MACE10 is a mobile UAC experiment, where Doppler induced temporal scaling effects (stretching or compression) are present. Temporal resampling is thus implemented to convert the Doppler scaling effects to Doppler frequency shifts. The channel model remained after the temporal resampling procedure is similar to that in the WHIO09 and ACOMM10 experiments. We compare the GoSLIM and GoSLIM-V algorithms in the channel estimation stage and compare the RELAX-BLAST scheme and the LMMSE Turbo equalization technique (including its low complexity approximation) in the symbol detection stage.

The structure of a transmitted data package is shown in Figure 9, which is similar to that of the ACOMM10 experiment. Each package consists of 4 packets which are designed to test the MIMO BLAST scheme. The 1st packet conveys a grayscale Gator mascot and the subsequent 3 packets combined form a colored mascot. The RGB components of the colored image were transmitted in the 2nd, 3rd, and 4th packets, respectively. Each packet is constructed as follows (see Figure 9): time-

marking sequences are placed at the beginning of each packet to facilitate the temporal resampling procedure; two guard intervals (each containing 500 silent symbols) are placed, respectively, before and after the segments containing the payload symbols and training sequences. The payload symbols contain the information of the Gator mascot image. By transmitting $N = 4$ sequences simultaneously and incorporating the measurements acquired from all of the $M = 12$ receiver elements for analysis, we established a 4×12 MIMO UAC system, which leads to a net coded data rate of 11.7 kbps. The data package was transmitted periodically and recorded by the receiver array. A total of 120 epochs were available and they are referred to as "E001"--"E120", respectively.

The packet is resampled using the Doppler scaling factor estimated by taking advantage of the time-marking sequences. To assess the performance of the resampling process, the CIR and Doppler frequency evolutions obtained by GoSLIM before we resample the 2nd packet of epoch "E002" are shown in Figures 10(a) and 10(c), respectively. In comparison, Figures 10(b) and 10(d) demonstrate the corresponding CIR and Doppler frequency evolutions obtained after resampling the packet, respectively. We can see from Figure 10 that the temporal resampling process successfully reduces the Doppler scaling effects to Doppler frequency shifts. Moreover, it is interesting to look at Figure 11 where the vessel speed estimated during the resampling stage is plotted on top of the GPS reference information provided by WHOI (the GPS device was equipped on the moving vessel). The good agreement between these two curves verifies the effectiveness of the resampling procedure we employ. The analysis presented hereafter is based on the resampled measurements.

Spatial multiplexing schemes: BLAST data

We choose the 1st packet of epoch "E018" to verify the channel model behind GoSLIM-V (other epochs give similar observations). The evolution of the Doppler frequencies produced by GoSLIM for all the 12 receive hydrophones are plotted superimposed in Figure 12 along with the evolution of the Doppler frequency obtained by GoSLIM-V. One observes that the curves show good agreement with each other, which verifies the validity of the key assumption for GoSLIM-V that different receivers experience the same Doppler frequency. We proceed to assess the impact of the channel estimation algorithm (GoSLIM or GoSLIM-V) on the resulting detection performance. With the estimated CIRs and Doppler frequency (frequencies), after phase compensation, the payload symbols are detected using the RELAX-BLAST scheme.

There is a total of 480 packets available and we deem a packet to be successfully detected if its coded BER is less than 0.1. When GoSLIM is employed as the channel estimation algorithm, we have succeeded in tracking the entire 32 payload blocks for 391 packets. A coded BER of 1.7×10^{-2} is achieved after averaging over the 391 successful packets. In comparison, when GoSLIM-V is used, 396 packets are successfully retrieved with an average coded BER of 1.6×10^{-2}. We use the 1st packet (i.e., the one conveys a grayscale gator mascot; see Figure 9) of three epochs, namely "E013", "E016", and "E018", to assess the impact of the two channel estimation algorithms on the resulting BER performance and computation complexity. When GoSLIM is employed, Figures 13(a), 13(b), and 13(c) show the recovered grayscale mascots for "E013", "E016", and "E018", respectively. The corresponding coded BERs and the computational time consumed at the channel estimation stage on an ordinary workstation (Intel Xeon E5506 processor 2.13G Hz, 12GB RAM, Windows 7 64-bit, and MATLAB R2010b) are listed in the first row of Tables 8 and 9, respectively. In comparison, when GoSLIM-V is employed, the recovered grayscale mascots are shown in Figures 13(d), 13(e), and 13(f), with the corresponding BERs and computational complexities listed in the second row of Tables 8 and

9, respectively. One observes from Table 8 that GoSLIM-V yields slightly better BER results than its GoSLIM counterpart. Moreover, Table 9 demonstrates that GoSLIM-V is about 4 times faster than GoSLIM. Due to the advantage of GoSLIM-V over the original GoSLIM algorithm, we hereafter employ GoSLIM-V in the channel estimation stage and compare the RELAX-BLAST scheme with the Turbo equalization counterpart in the symbol detection stage.

Table 10 lists the successfully detected packet percentage, the error-free packet percentage, the coded BER averaged over the successful packets, and the time ratio of the time consumed to process a packet to the duration of the same packet during transmission, obtained using Exact-LMMSE-Turbo, Approximate-LMMSE-Turbo, and the RELAX-BLAST scheme, respectively. The results are obtained by applying 3 iterations for all of the three types of detection schemes considered. Similar observations can be obtained from Table 10 as from Table 7 in the ACOMM10 experimental results. Moreover, we analyze epoch "E054" that leads to perfect recovery of both the grayscale and colored mascots (see Figure 14(b) and 14(d)) using either Exact-LMMSE-Turbo or Approximate-LMMSE-Turbo. In comparison, the grayscale and colored mascots recovered from epoch "E054" using RELAX-BLAST are shown in Figures 14(a) and 14(c), respectively, with the corresponding coded BERs being 1.8×10^{-1} and 1.6×10^{-1}.

IMPACT/APPLICATIONS

The natural bandwidth limitations of coherent underwater acoustic channel suggest a technical breakthrough. MIMO signal processing is a promising bandwidth efficient method to high data rate and high quality services. Our promising results are expected to favorably impact high-rate long-range MIMO-UAC designs.

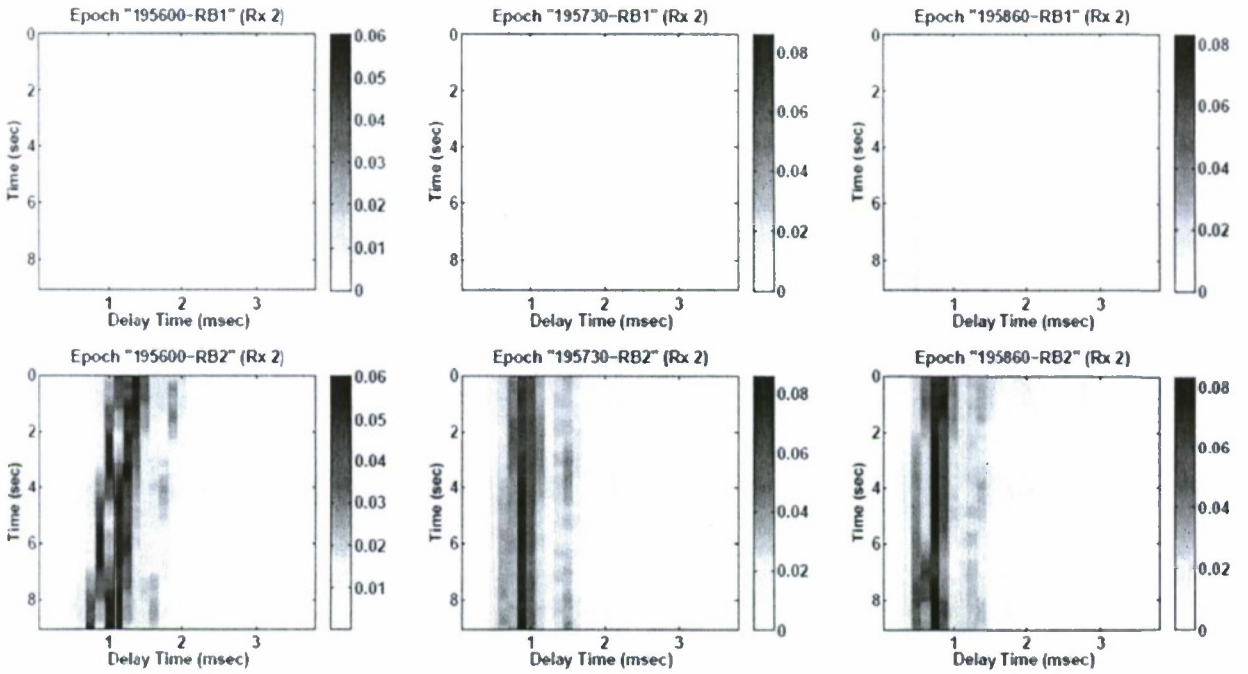

Figure 1: CIR evolution over approximately a 9 second period at the 2nd receiver for all the 6 epochs. [graph: One observes from the GoSLIM CIR estimates that the position of the principal arrival shifts with time. This observation is in line with the fact that the transmitter array was suspended from a vessel heaving in a 14 m mid-depth water column and the receiving hydrophone arrays were mounted on anchored buoys during the course of data collection in WHOI09 in-water experiment.]

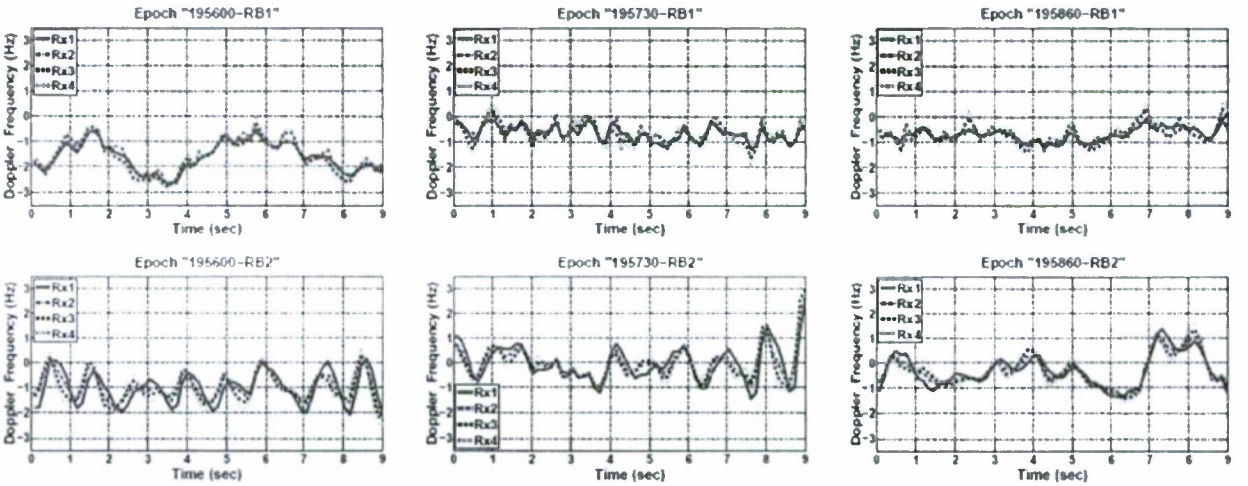

Figure 2: Evolution of the estimated Doppler frequencies at each receiver for all the 6 epochs. [graph: The reverberating Doppler frequency estimates obtained from the GoSLIM algorithm provide evidence on the presence of Doppler shifts.]

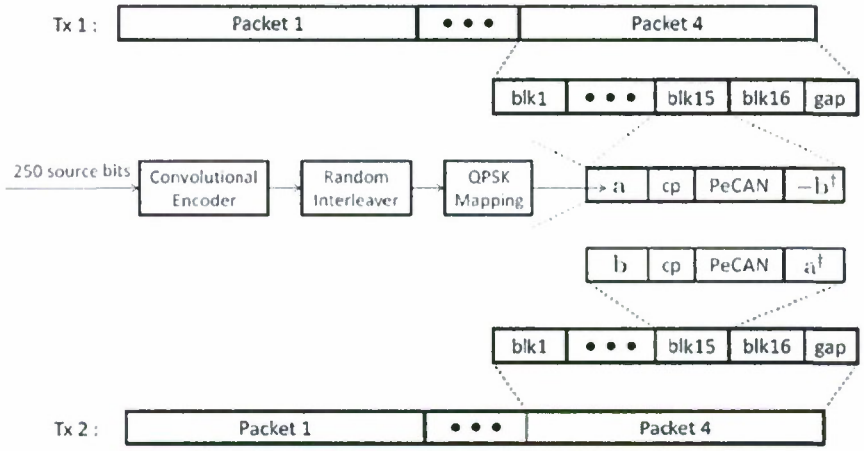

Figure 3: The structure of the transmitted sequence using 2Tx-1Rx Alamouti scheme. [graph: Each transmitter sends 4 data packets and each packet is divided into 16 blocks. The payload symbols contained in each block are constructed using Alamouti diversity scheme.]

	RB1		RB2	
	uncoded BER	coded BER	uncoded BER	coded BER
Rx1	2.7083×10^{-4}	0	1.8750×10^{-4}	0
Rx2	0.0180	0.0021	1.2500×10^{-4}	0
Rx3	1.6146×10^{-4}	0	6.2498×10^{-5}	0
Rx4	3.2291×10^{-4}	0	1.1458×10^{-4}	0

Table 1: Coded and uncoded BER performance of GoSLIM coupled with Alamouti diversity scheme for 2Tx-1Rx system.
[graph: GoSLIM coupled with Alamouti diversity scheme yields satisfactory detection performance except for the 2^{nd} hydrophone of RB1 receiving array. The reason is that the estimated channel power of this hydrophone is persistently lower than those of other hydrophones by almost an order of magnitude, see Figure 1.]

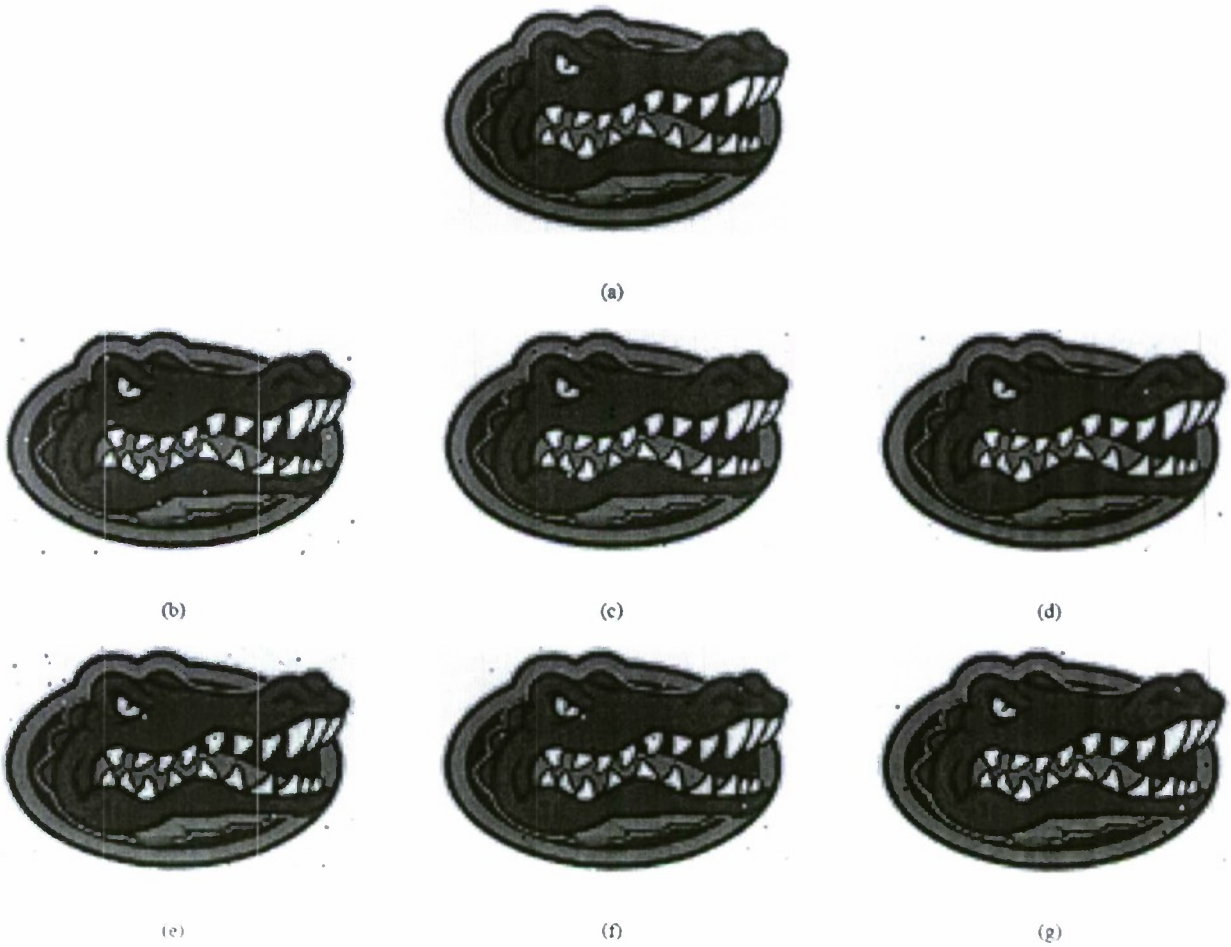

Figure 4: (a) The grayscale Gator mascot transmitted (truth). (b) Mascot recovered from Epoch "195600-RB2". (c) Mascot recovered from Epoch "195730-RB2". (d) Mascot recovered from Epoch "195860-RB2". (e) Mascot recovered from Epoch "195600-RB2". (f) Mascot recovered from Epoch "195730-RB2". (g) Mascot recovered from Epoch "195860-RB2". (b)-(d) are obtained by GoSLIM. (e)-(g) are obtained by GoSLIM-V.

	195600	195730	195860
GoSLIM	2.0×10^{-3}	9.7×10^{-4}	7.2×10^{-4}
GoSLIM-V	1.8×10^{-3}	8.1×10^{-4}	5.9×10^{-4}

Table 2: Coded BER results obtained by GoSLIM and GoSLIM-V, respectively.

	195600	195730	195860
GoSLIM (15 iterations)	38.6	39.6	40.1
GoSLIM-V (15 iterations)	10.5	10.7	10.8

Table 3: Complexity comparison (in second) between GoSLIM and GoSLIM-V.

	195600	195730	195860
Exact-LMMSE-Turbo (3 iterations)	512.0	513.3	514.0
Approximate-LMMSE-Turbo (3 iterations)	21.9	22.3	22.5
RELAX-BLAST (3 iterations)	19.8	20.0	20.5

Table 4: The time ratio summary of Exact-LMMSE-Turbo, Approximate- LMMSE-Turbo, and RELAX-BLAST.

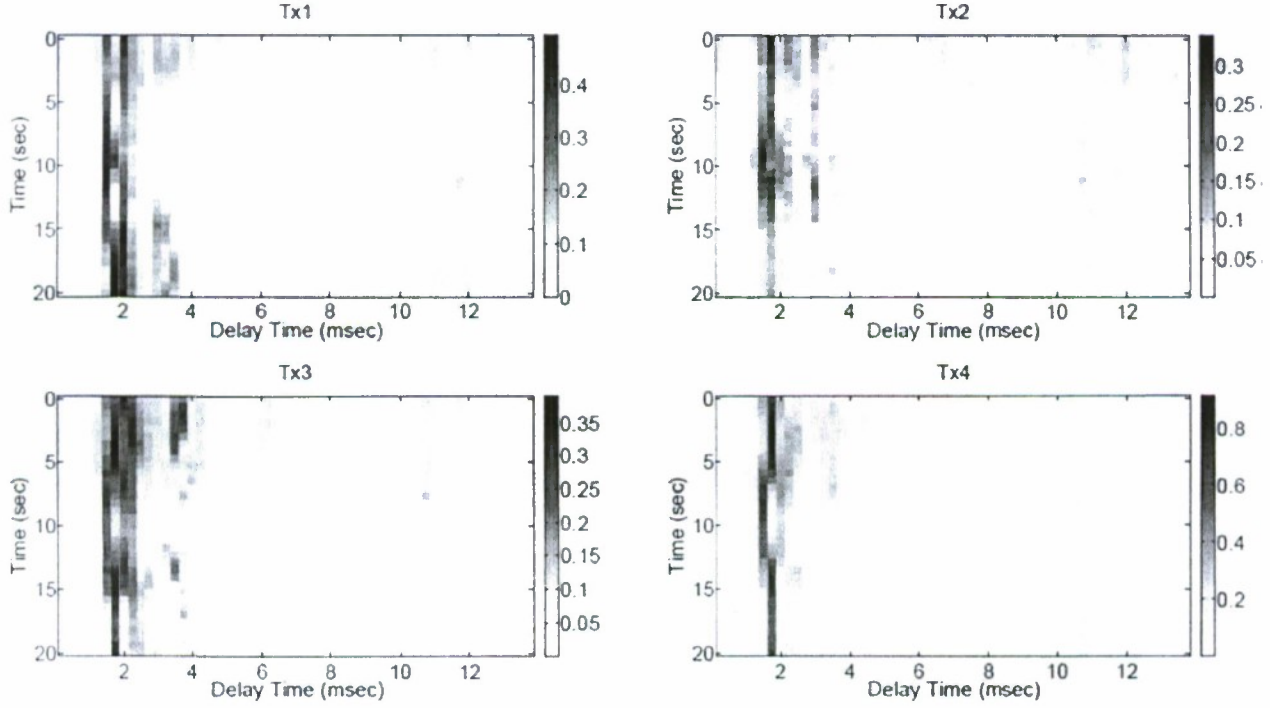

Figure 5: CIR evolutions obtained by GoSLIM between the four active transmitters and one hydrophone for Epoch "MIMO28".

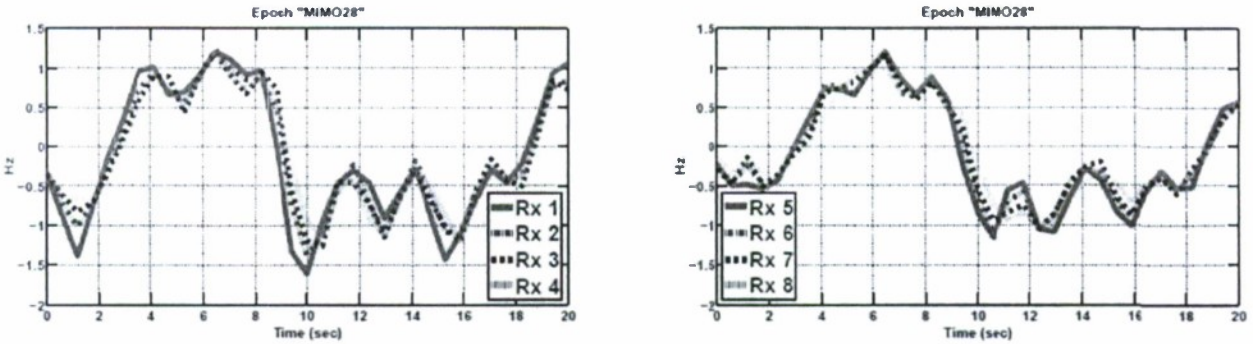

Figure 6: Evolutious of the Doppler frequencies estimated by GoSLIM at each receiver for Epoch "MIMO28".

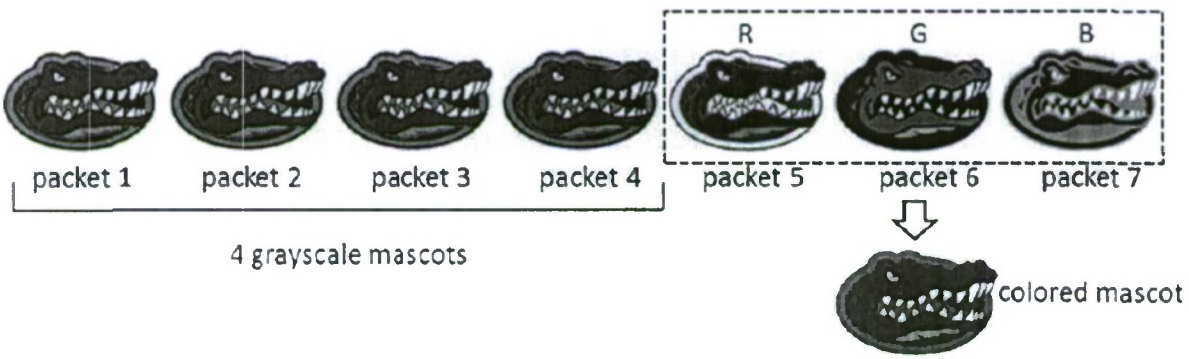

Figure 7: Each package transmitted in the ACOMM10 experiment contains 4 grayscale Gator mascot images and 1 colored image. The colored image is decomposed into RGB components.

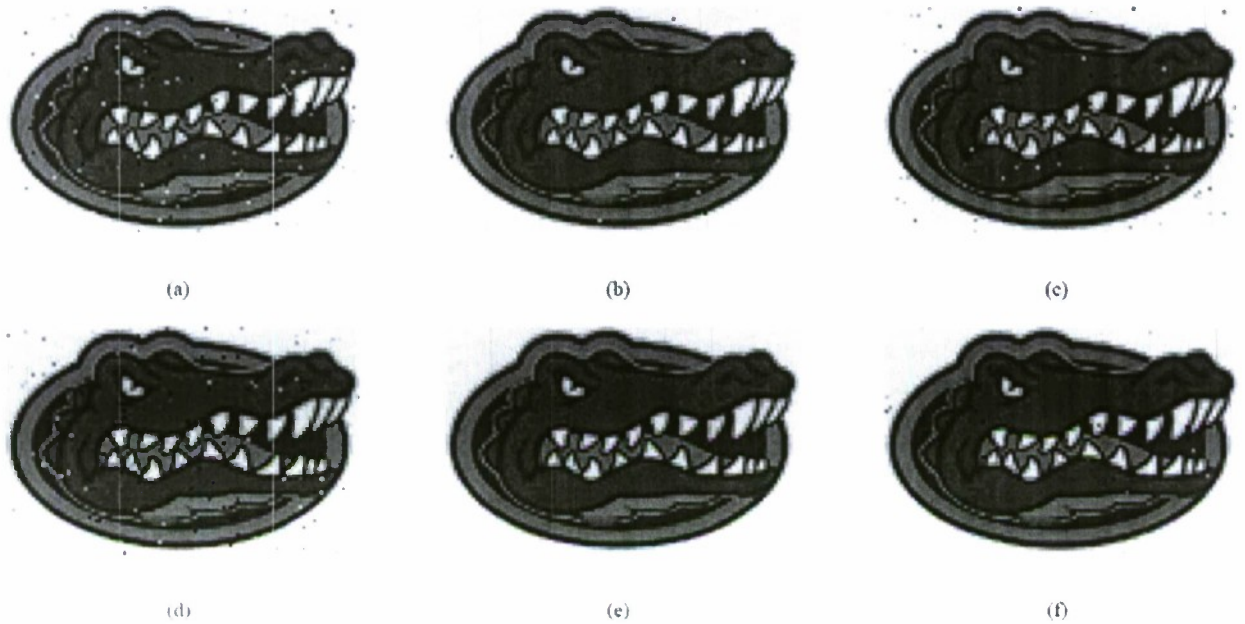

Figure 8: (a) Grayscale mascot recovered from epoch "MIMO02". (b) Grayscale mascot recovered from epoch "MIMO06". (c) Grayscale mascot recovered from epoch "MIMO18". (d) Grayscale mascot recovered from epoch "MIMO02". (e) Grayscale mascot recovered from epoch "MIMO06". (f) Grayscale mascot recovered from epoch "MIMO18". (a)-(c) are obtained by GoSLIM. (d)-(f) are obtained by GoSLIM-V.

	MIMO02	MIMO06	MIMO18
GoSLIM	6.2×10^{-3}	7.8×10^{-4}	3.9×10^{-3}
GoSLIM-V	5.4×10^{-3}	6.3×10^{-5}	1.2×10^{-3}

Table 5: Coded BER results obtained by GoSLIM and GoSLIM-V, respectively.

	MIMO02	MIMO06	MIMO18
GoSLIM (15 iterations)	82.0	81.3	83.1
GoSLIM-V (15 iterations)	21.4	20.5	21.2

Table 6: Complexity comparison (in second) between GoSLIM and GoSLIM-V.

	successful packet percentage (%)	error-free packet percentage (%)	average coded BER	time ratio
Exact-LMMSE-Turbo (3 iterations)	100	100	0	442.7
Approximate-LMMSE-Turbo (3 iterations)	100	97.9	1.6×10^{-5}	15.2
RELAX-BLAST (3 iterations)	95.3	8.7	5.1×10^{-3}	14.5

Table 7: The performance summary of Exact-LMMSE-Turbo, Approximate- LMMSE-Turbo, and RELAX-BLAST.

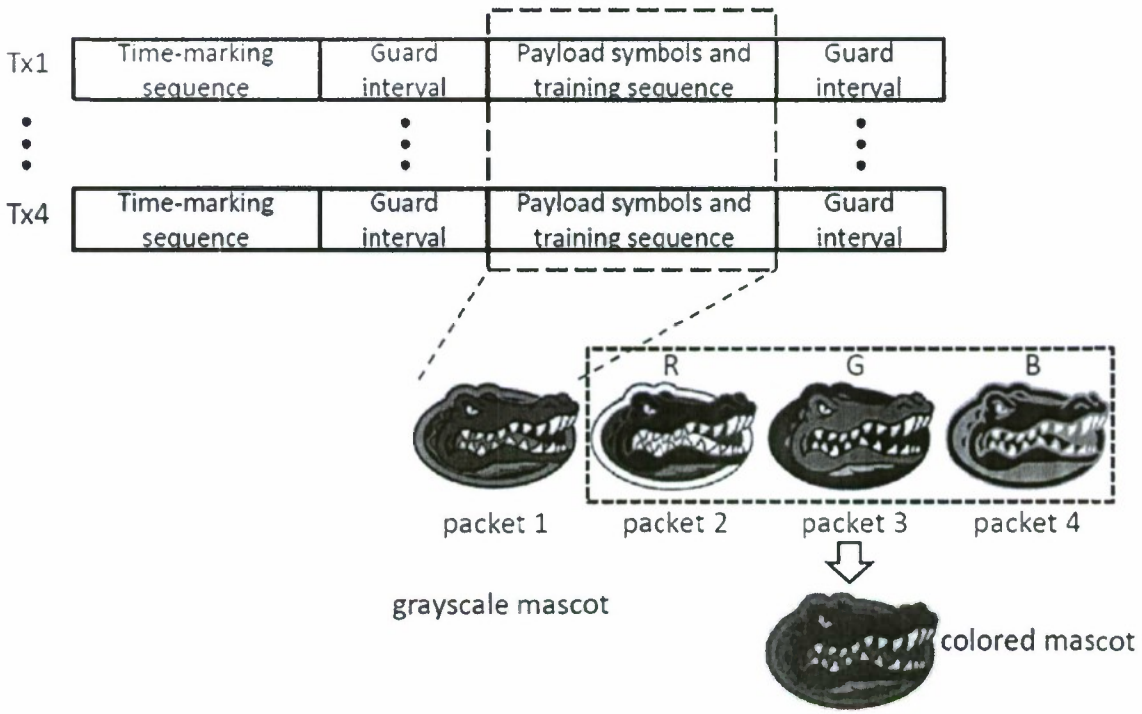

Figure 9: The structure of the package used in the MACE10 experiment.

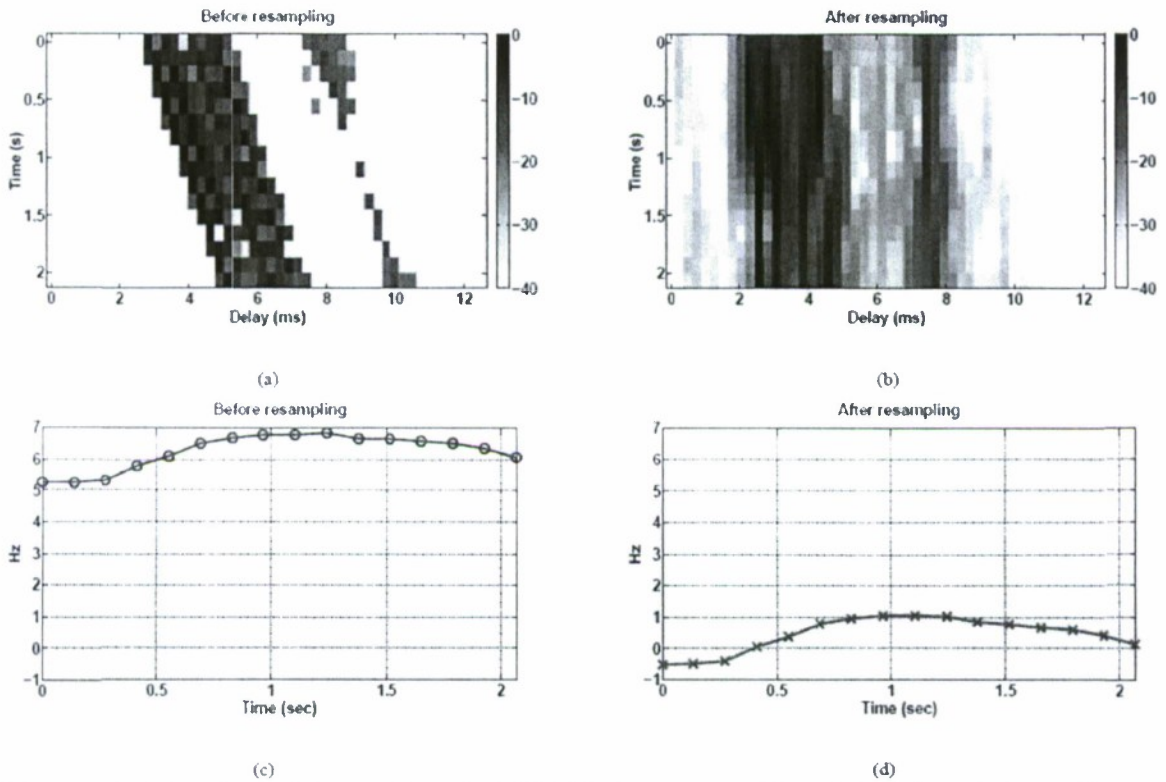

Figure 10: (a) CIR evolution of Epoch "E002" before resampling. (b) CIR evolution of Epoch "E002" after resampling. (c) Doppler frequency evolution of Epoch "E002" before resampling. (d) Doppler frequency evolution of Epoch "E002" after resampling.

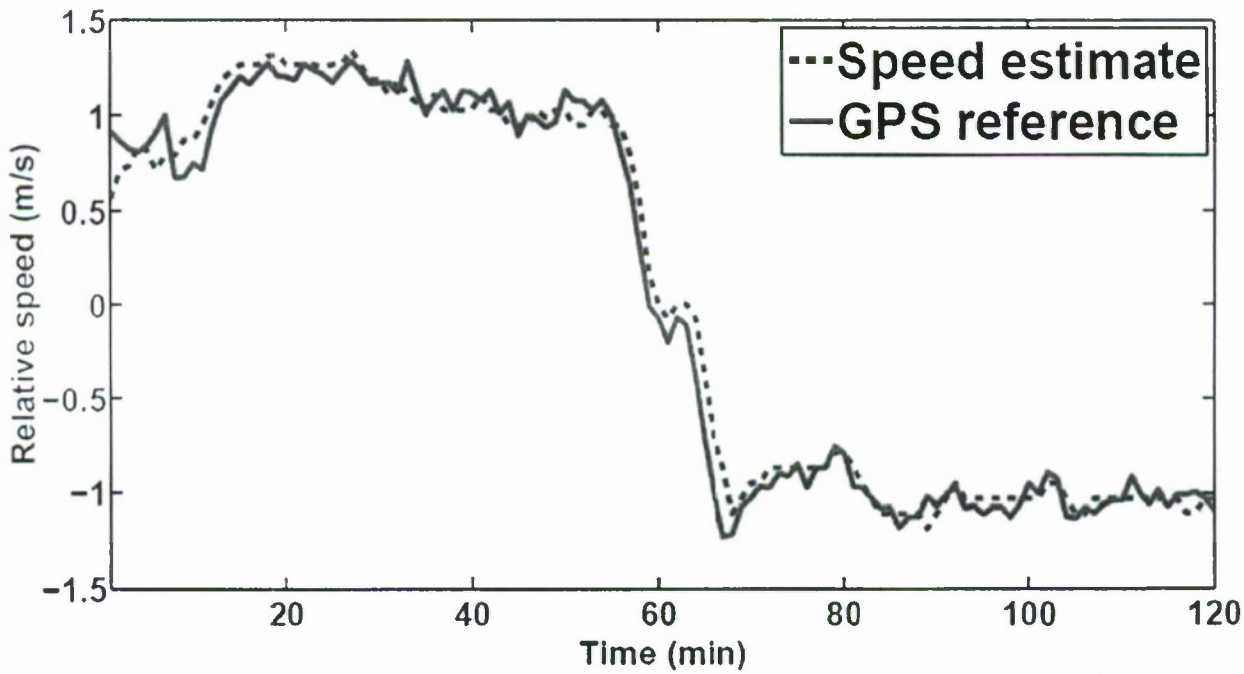

Figure 11: The relative speed between the transmitter and receiver array given by GPS and estimated during the temporal resampling stage (courtesy of Milica Stojanovic's group).

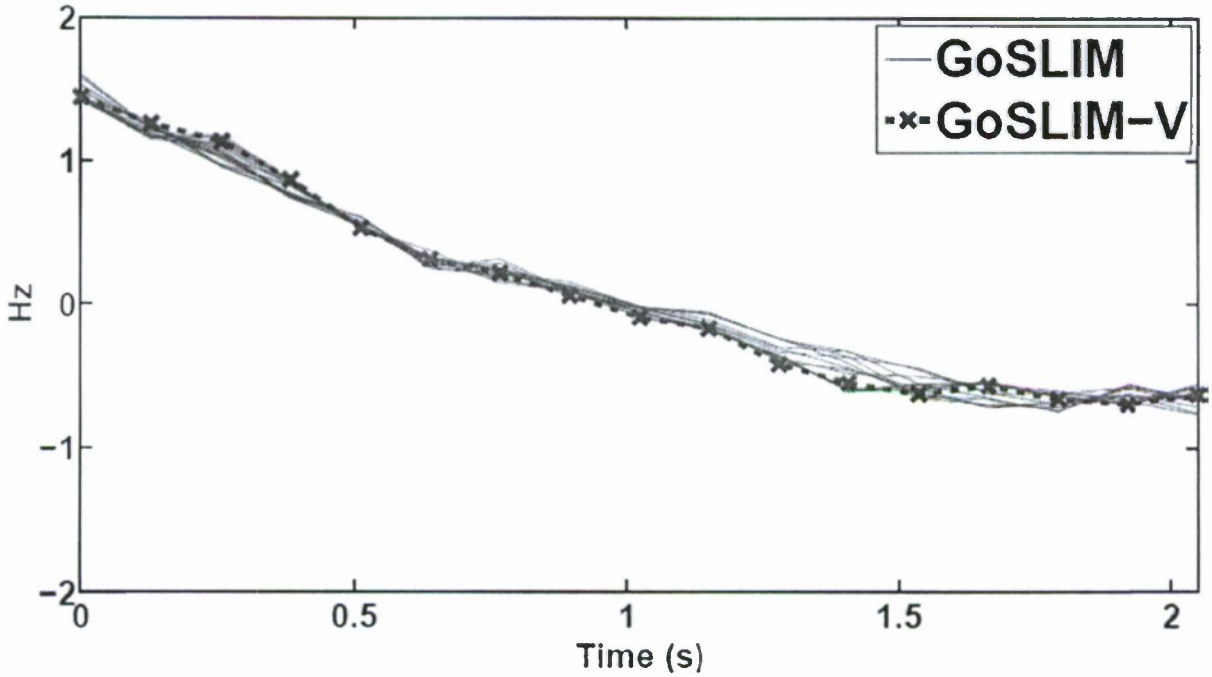

Figure 12: Doppler frequency evolution of the first packet in epoch "E018" obtained by GoSLIM and GoSLIM-V, respectively.

	E013	E016	E018
GoSLIM	3.6×10^{-2}	3.6×10^{-3}	1.6×10^{-4}
GoSLIM-V	2.3×10^{-2}	3.1×10^{-3}	9.4×10^{-5}

Table 8: Coded BER results obtained by GoSLIM and GoSLIM-V, respectively.

	E013	E016	E018
GoSLIM (15 iterations)	122.8	121.1	123.0
GoSLIM-V (15 iterations)	32.1	31.8	32.3

Table 9: Complexity comparison (in second) between GoSLIM and GoSLIM-V.

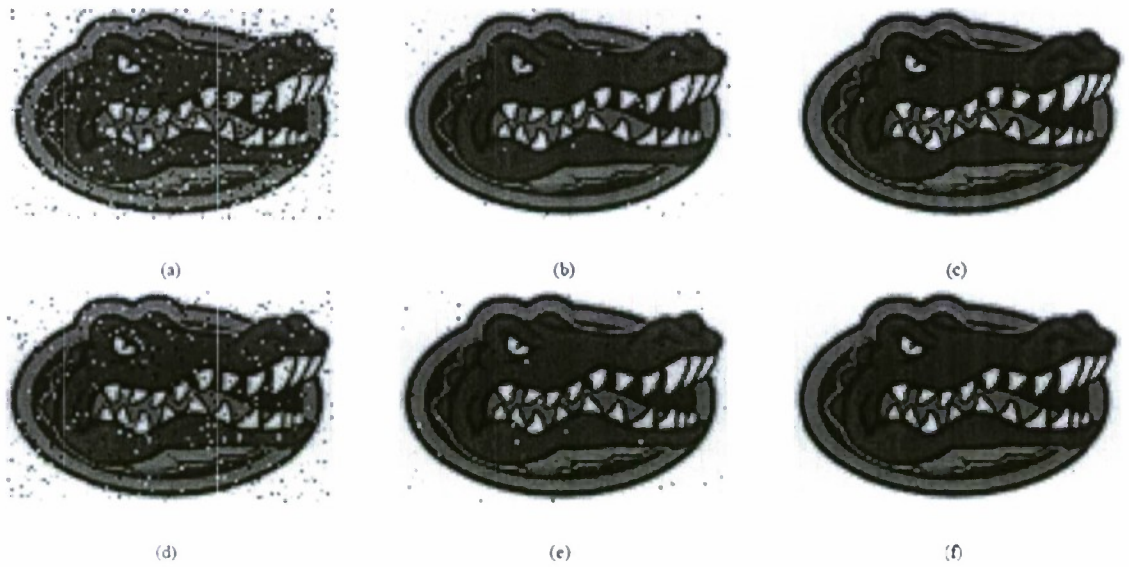

Figure 13: (a) Grayscale mascot recovered from epoch "E013". (b) Grayscale mascot recovered from epoch "E016". (c) Grayscale mascot recovered from epoch "E018". (d) Grayscale mascot recovered from epoch "E013". (e) Grayscale mascot recovered from epoch "E016". (f) Grayscale mascot recovered from epoch "E018". (a)-(c) are obtained by GoSLIM. (d)-(f) are obtained by GoSLIM-V.

	successful packet percentage (%)	error-free packet percentage (%)	average coded BER	time ratio
Exact-LMMSE-Turbo (3 iterations)	100	76.7	9.2×10^{-5}	488.1
Approximate-LMMSE-Turbo (3 iterations)	100	74.4	2.1×10^{-4}	17.2
RELAX-BLAST (3 iterations)	82.5	4.8	1.6×10^{-2}	16.9

Table 10: The performance summary of Exact-LMMSE-Turbo, Approximate- LMMSE-Turbo, and RELAX-BLAST.

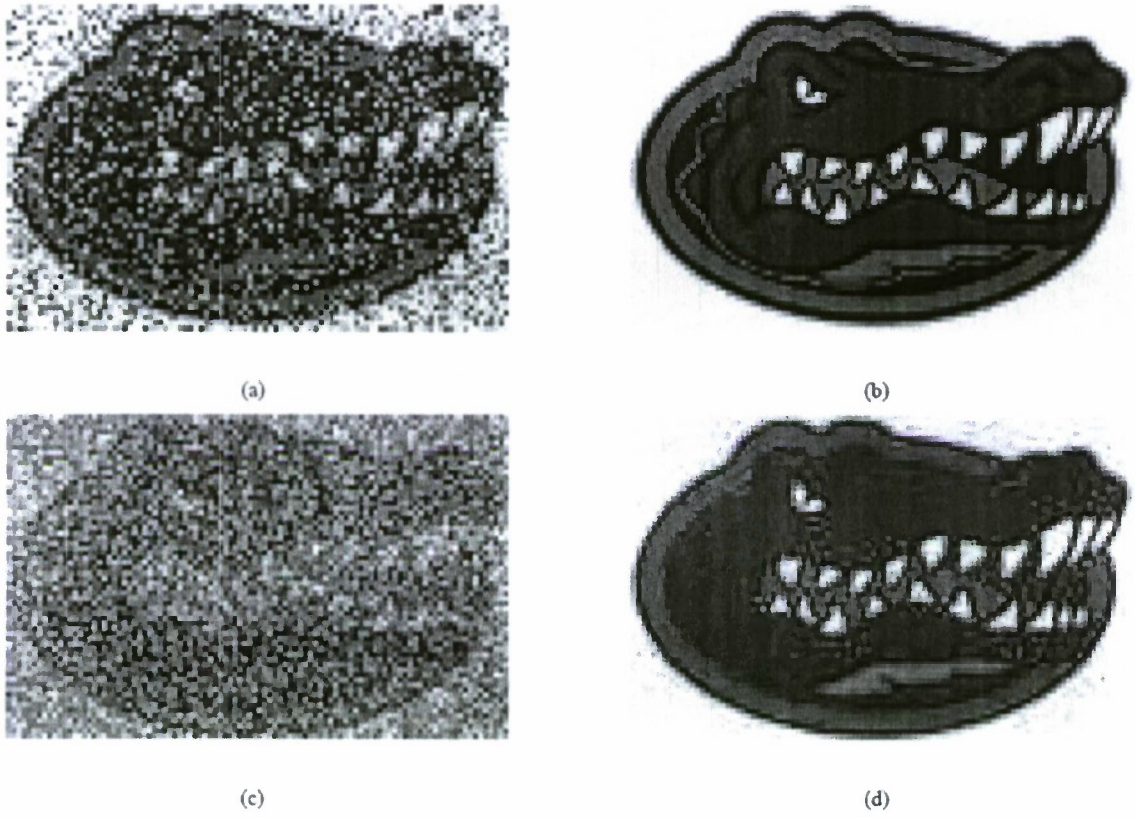

Figure 14: (a) Grayscale mascot recovered from epoch "E054" using RELAX-BLAST. (b) Grayscale mascot recovered from epoch "E054" using Turbo equalization. (c) Colored mascot recovered from epoch "E054" using RELAX-BLAST. (d) Colored mascot recovered from epoch "E054" using Turbo equalization.

PUBLICATIONS

Journal

1. J. Ling, H. He, J. Li, W. Roberts, and P. Stoica, "Covert Underwater Acoustic Communications," *Journal of the Acoustical Society of America*, vol. 128, no. 5, pp. 2898-2909, November 2010. [published, refereed]
2. X. Tan and J. Li, "Cooperative Positioning in Underwater Sensor Networks," *IEEE Transactions on Signal Processing*, vol. 58, no. 11, pp. 5860-5871, November 2010. [published, refereed]
3. P. Stoica, P. Babu, and J. Li, "New Method of Sparse Parameter Estimation in Separable Models and Its Use for Spectral Analysis of Irregularly Sampled Data," *IEEE Transactions on Signal Processing*, vol. 59, no. 1, pp. 35 – 47, January 2011. [published, refereed]
4. H. He, P. Stoica, and J. Li, "Wideband MIMO Systems: Signal Design for Transmit Beampattern Synthesis," *IEEE Transactions on Signal Processing*, vol. 59, no. 2, pp. 618-628, February 2011. [published, refereed]

5. J. Ling, K. Zhao, J. Li, and M. L. Nordenvaad, "Multi-input multi-output underwater communications over sparse and frequency modulated acoustic channels," *Journal of the Acoustical Society of America,* vol. 130, no. 1, pp. 249-262, July 2011. [published, refereed]
6. J. Ling, X. Tan, T. Yardibi, J. Li, M. L. Nordenvaad, H. He, and K. Zhao, "On Bayesian channel estimation and FFT based symbol detection in MIMO underwater acoustic communications," *IEEE Journal of Oceanic Engineering.* [submitted]
7. J. Ling and J. Li, "Gibbs sampler based semi-blind equalizer in underwater acoustic communications," *IEEE Journal of Oceanic Engineering.* [submitted]
8. K. Zhao, J. Ling and J. Li, "Mobile multi-input multi-output underwater acoustic communications," *Journal of the Acoustical Society of America.* [submitted]

Conference

1. H. He, P. Stoica, and J. Li, "Wideband MIMO Waveform Design for Transmit Beampattern Synthesis," *IEEE 5th International Waveform Diversity & Design Conference*, Niagara Falls, Canada, August 8-13, 2010. [published, refereed]
2. J. Ling, H. He, J. Li, P. Stoica, and W. Roberts, "Covert underwater acoustic communications: Transceiver structures, waveform designs and associated performances," *Proceedings of MTS/IEEE Oceans Conference*, Seattle, WA, September 2010. [published, refereed]
3. X. Tan and J. Li, "Cooperative positioning in underwater sensor networks," *Proceedings of MTS/IEEE Oceans Conference*, Seattle, WA, September 2010. [published, refereed]
4. J. Ling, X. Tan, J. Li, and M. L. Nordenvaad, "Efficient channel equalization for MIMO underwater acoustic communications," *Proceedings of 6th Sensor Array and Multichannel Signal Processing Workshop*, Ma'ale Hahamisha, Israel, October 2010. [published, refereed]
5. H. He, P. Stoica, and J. Li, "On Synthesizing Cross Ambiguity Functions," *IEEE International Conference on Acoustics, Speech and Signal Processing*, Prague, Czech Republic, May 22-27, 2011. [published, refereed]
6. K. Zhao, J. Ling, and J. Li, "Mobile multi-input multi-output underwater acoustic communications," *Proceedings of IEEE Oceans Conference*, Santander, Spain, June 2011. [published, refereed]
7. K. Zhao, J. Ling, and J. Li, "On estimating sparse and frequency modulated channels for MIMO underwater acoustic communications," *Proceedings of 2011 Allerton Conference on Communication, Control, and Computing* (invited), Monticello, IL, USA, September 2011. [in press]
8. K. Zhao, J. Ling, and J. Li, "On Turbo equalization for MIMO underwater acoustic communications," *Proceedings of 163rd Meeting of the Acoustical Society of America* (invited), Hong Kong, May 2012. [in press]